Synthesis and Characterization of $Ba_3Bi_{6.67}Se_{13}$ and Its Filled Variants $Ba_3Bi_6PbSe_{13}$ and $Ba_3Bi_6SnSe_{13}$

Ying C. Wang and Francis J. DiSalvo*

Department of Chemistry and Chemical Biology, Baker Laboratory, Cornell University, Ithaca, New York 14853

Received September 7, 1999. Revised Manuscript Received January 3, 2000

The three title compounds were synthesized at 710 °C and their structure type is isotypic to $Sr_4Bi_6Se_{13}$ and β-$K_2Bi_8Se_{13}$. The compounds crystallize in $P2_1/m$ ($Z = 2$) with $a = 17.2228(6)$ Å, $b = 4.2729(1)$ Å, $c = 18.4659(6)$ Å, $\beta = 90.720(0)°$ for $Ba_3Bi_{6.67}Se_{13}$; $a = 17.2427(4)$ Å, $b = 4.2736(1)$ Å, $c = 18.4560(4)$ Å, $\beta = 90.861(1)°$ for $Ba_3Bi_6PbSe_{13}$; and $a = 17.2498(5)$ Å, $b = 4.2912(1)$ Å, $c = 18.4590(5)$ Å, and $\beta = 90.679(1)°$ for $Ba_3Bi_6SnSe_{13}$. The coordination environments of Bi/Pb/Sn are distorted Se octahedra, while the coordination spheres of Ba are bi- or tricapped trigonal prisms. Transport measurements indicate that $Ba_3Bi_{6.67}Se_{13}$ and $Ba_3Bi_6PbSe_{13}$ are semiconducting.

1. Introduction

Recently there has been increasing interest in searching for semiconductors as thermoelectric materials with high figures of merit $ZT = S^2T/\rho\kappa$ (>1). Some empirical guides on searching for good thermoelectric materials are systems with heavy elements that have small electronegativity differences, a large unit cell, high coordination numbers, high dielectric constant, a band gap around 10 k_BT, and high crystal symmetry.[1] Recent research has focused on skutterudites, chalcogenides, and clathrates among others.[2] Since $Bi_{2-x}Sb_xTe_{3-y}Se_y$ alloys are the best thermoelectric materials at room temperature so far,[3] complex chalcogenides with structural modifications based on Sb_2Q_3 and Bi_2Q_3 (Q= Se and Te) are reasonable candidates. Some ternary Bi/Sb-containing chalcogenides display high thermopower, high electrical conductivity, and low thermal conductivity, which makes them promising thermoelectric materials.[4]

There have been many reports on the synthesis and properties of alkali metal Bi/Sb chalcogenides, but there are many fewer reports of alkaline earth metal Bi/Sb chalcogenides.[4] The powerful method of using molten alkali metal polychalcogenides[5,6] as fluxes cannot be simply applied to the synthesis of alkaline earth metal containing Bi/Sb chalcogenides, especially when the incorporation of alkali metals is not desired. Furthermore, the control of compound purity is very important to thermoelectric applications, since the transport properties are very sensitive to the impurity determined carrier densities.

This work reports the synthesis of $Ba_3Bi_{6.67}Se_{13}$, $Ba_3Bi_6PbSe_{13}$, and $Ba_3Bi_6SnSe_{13}$ through direct combination and their structural and electronic properties.

2. Experimental Section

Reagents. All the chemicals in this work were used as obtained: barium distilled dendritic pieces, 99.9+% purity, ampuled under argon, Aldrich, Milwaukee, WI; selenium pellets, 99.9999% purity, Atomergic Chemetals Corp., Plainview, NY; bismuth powder, 99.999% purity, −8 mesh, Alfa Products, Danvers, MA; tin shots, 99.999% purity, Strem Chemicals, Newburyport, MA; lead bars, 99.999% purity, Johnson Matthey Electronics, Inc., Spokane, WA.

Synthesis. Due to the air sensitivity of barium, all work was carried out under an argon atmosphere in a vacuum-dry box. $Ba_3Bi_{6.67}Se_{13}$ was originally synthesized from a mixture of 0.1053 g of Ba, 0.6409 g of Bi, and 0.4238 g of Se with the stoichiometry Ba:Bi:Se::1:4:7. The elemental mixture was put in a vitreous carbon crucible and was sealed in an evacuated quartz tube. Then it was gradually heated to 710 °C over 48 h, kept at that temperature for 100 h, and slowly cooled to 510 °C at 2 °C/h. Powder X-ray diffraction patterns (Scintag XDS 2000 with Cu Kα radiation) of the black shiny product showed peaks corresponding to Bi_2Se_3 and other peaks that could not be indexed to any known phases. Microprobe analysis (JEOL 733) suggested that two phases exist in the product: one is Bi_2Se_3 and the other one is a ternary phase with the approximate ratio Ba:Bi:Se::1.0:2.4:4.4. A needlelike crystal was obtained from the product mixture and used for single-crystal diffraction study, which yielded the formula $Ba_3Bi_{6.67}$-

* Corresponding author. Phone: 607-255-7238. Fax: 607-255-4137. E-mail: fjd3@cornell.edu.

(1) (a) DiSalvo, F. J. *Science* **1999**, *285*, 703. (b) Mahan, G.; Sales, B.; Sharp, J. *Physics Today* **1997**, March, *50*, 42. (c) Wood, C. *Rep. Prog. Phys.* **1988**, *51*, 459. (d) Rowe, D. M.; Bhandari, C. M. *Modern Thermoelectrics*; Reston Publishing Company, Inc.: Virginia, 1983.

(2) MRS 1998 Fall Meeting, Boston, MA, *Thermoelectric Materials*, MRS 1998 Fall Meeting, Boston, MA; Materials Research Society: Warrendale, PA, 1998; p 477f.

(3) (a) *Encyclopedia of Materials Science and Engineering, Thermoelectric Semiconductors*; MIT Press: Cambridge, MA; p 4968. (b) Goldsmid, H. J. *Electric Refrigeration*; Pion: London, 1986; p 88.

(4) (a) Chung, D.-Y.; Choi, K.-S.; Iordanidis, L.; Schindler, J. L.; Brazis, P. W.; Kannewurf, C. R.; Chen, B.; Hu, S.; Uher, C.; Kanatzidis, M. G. *Chem. Mater.* **1997**, *9*, 3060. (b) Chung, D.-Y.; Iordanidis, L.; Choi, K.; Kanatzidis, M. G. *Bull. Korean Chem. Soc.* **1998**, *19*, 1283. (c) Chung, D.-Y.; Jobic, S.; Hogan, T.; Kannewurf, C. R.; Brec, R.; Rouxel, J.; Kanatzidis, M. G. *J. Am. Chem. Soc.* **1997**, *119*, 2505. (d) Iordanidis, L.; Brazis, P. W.; Kannewurf, C. R.; Kanatzidis, M. G. *Thermoelectric Materials* 1998 − *The Next Generation Materials for Small-Scale Refrigeration and Power Generation Applications*; Tritt, T. M., Kanatzidis, M. G., Mahan, G. D., Lyon, H. B., Jr., Eds. *Mater. Res. Soc. Symp. Proc.* **1999**, *545*, 189.

(5) Kanatzidis, M. G.; Sutorik, A. *Prog. Inorg. Chem.* **1995**, *43*, 151.

(6) Sunshine, S. A.; Kang, D.; Ibers, J. A. *J. Am. Chem. Soc.* **1987**, 109, 6202.

10.1021/cm990571u CCC: $19.00
Published on Web 03/25/2000

Se_{13}. Afterward, it was found that a pure single phase can be obtained by heating a stoichiometric mixture of Ba:Bi:Se::3:6.67:13 to 710 °C or higher temperatures. In a similar way, pure phases $Ba_3Bi_6PbSe_{13}$ and $Ba_3Bi_6SnSe_{13}$ were synthesized by heating stoichiometric mixtures of elements to 710 °C or higher temperatures.

Transport Property Measurements. The electrical resistivity was measured on a home-built apparatus by using four-probe ac techniques.[7] Current contacts were made by attaching 0.05-mm-thick copper foil strips at the ends of each sample with silver epoxy (H20E, Epoxy Technology). Voltage leads were made by placing 38 AWG copper wires coated with silver epoxy on the flat surfaces of each sample bar. A ±10% error in absolute value of resistivity is possible due to uncertainties in measuring the area factor and the voltage contact spacing.[7]

The thermopower was measured on the sample using the steady-state technique in a home-built setup.[7] The sample was first mounted on a copper base with silver epoxy. A 5 kΩ resistor (heater) was attached to the opposite end of the sample with silver epoxy. Two 40 AWG Au,Fe(0.07%):Chromel-p thermocouples were attached to the epoxy joints at either end of the sample. The sample chamber was then evacuated to less than 4×10^{-5} Torr. Small and steady temperature gradients (maximum 2 K) were achieved by incrementally increasing the power to the resistor. The resulting temperatures on both ends of the sample were measured using the two attached thermocouples. The voltage across the sample was measured using the Chromel-p wires of the two thermocouples. From a plot of the voltage across the sample versus the temperature gradient, a slope could be calculated which is equal to the thermopower of the sample plus the thermopower of the Chromel-p wire. The absolute thermopower of the Chromel-p wire was subtracted from the measured slope to give the absolute thermopower of the sample. The overall accuracy of the thermopower measurement has been estimated from standards to be within ±5%.[7]

Measurements were conducted on sintered pellets of polycrystalline $Ba_3Bi_{6.67}Se_{13}$ and $BaBi_6PbSe_{13}$. The samples were synthesized at 780 °C for $Ba_3Bi_{6.67}Se_{13}$ and 910 °C for $BaBi_6PbSe_{13}$, then cooled to room temperature, ground and pressed into pellets under argon atmosphere, and sintered at 540 °C for 90 h. The pellets were cut into rectangular parallelepipeds (3.6 mm × 4.2 mm × 5.7 mm for $Ba_3Bi_{6.67}Se_{13}$ and 4.0 mm × 4.0 mm × 3.2 mm for $Ba_3Bi_6PbSe_{13}$). Phase purity was checked by powder X-ray diffraction (Scintag XDS 2000 with Cu Kα radiation).

Using the standard four-probe method, the Hall coefficient of the polycrystalline sample of $Ba_3Bi_6PbSe_{13}$ was measured at room temperature. It was cut to the dimensions 0.85 mm × 3.4 mm × 5.0 mm using a diamond-impregnated string saw. The current contacts at the opposite ends of the sample (5.0 mm apart) were made by attaching 0.05-mm-thick copper foil strips using silver epoxy (EPOTEK H20E). The voltage leads at two transverse spots (3.4 mm apart) were made by placing 34 AWG copper wires coated with silvery epoxy. A Linear Research LR-700 AC resistance bridge supplied a 10 mA current at 16 Hz to the sample, and its resistance was measured repeatedly in 0 and 1237 G magnetic fields. To correct for magnetoresistive contributions to the Hall resistance, the resistance changes in forward and reverse fields were averaged.

Electron Microscopy. Electron microprobe analysis of the compounds was conducted with a JEOL 733 or a JAX 8900R Superprobe. The accelerating voltage was 15 kV for energy dispersive spectroscopy (EDS) analysis and 20 kV for wavelength dispersive spectroscopy (WDS) analysis. Semiquantitative EDS analysis yielded the ratio Ba:Bi/Pb:Se::1.0:2.4:4.3. Since EDS could not distinguish between Pb and Bi, WDS equipped with PETH, PETJ, and TAP analyzing crystals was used to distinguish between Pb and Bi. Semiquantitative WDS analysis on the flat surfaces of $Ba_3Bi_6PbSe_{13}$ crystals revealed that the specimen had the ratio of Bi to Pb as 6.1 ± 0.2 (average of five data acquisitions). Semiquantitative EDS analysis on the flat surfaces of several crystals $Ba_3Bi_6SnSe_{13}$ revealed that the specimen had Ba:Bi:Sn:Se::1.0:1.8:0.3:3.6.

Crystallographic Study. Crystals of each compound were selected under a microscope and mounted on glass fibers by using extra fast setting epoxy (Hardman) for the room-temperature data collection or poly(butenes) (viscosity at 99 °C 109−125 cst, *d* 0.885, catalog no. 38868-8, Aldrich) for data collection at low temperatures. X-ray diffraction data sets were collected on a Bruker SMART diffractometer equipped with a 1 K CCD detector and a 3 kW sealed tube X-ray generator (Mo Kα, 30 s exposure time, $\Delta\omega = 0.3°$). No intensity decay was observed during the data collection for any crystals. The unit cells were refined during the integration (program SAINT) based on all strong reflections. The structure solution and refinement were carried out by using SHELXL-93 and SHELXL-97.[8] The PLATON software package[9] was run to check for possible higher lattice symmetry or missed additional symmetry. The program SADABS[10] was applied to conduct an empirical absorption correction. PSI scan and analytical absorption corrections by using XPREP[8] were attempted but they did not improve the refinement. As the crystals are thin needles and the compounds contain heavy elements, absorption for some reflections turns out to be severe. Disorder or nonstoichiometry in these compounds was reported to exist in isostructural compounds,[4a,11a,12] which may be one reason for the high residues. We surveyed several isostructural compounds.[4a,11a,12] Relatively high values of R/R_w or R_1/wR_2 are not uncommon: β-$K_2Bi_8Se_{13}$ with R/R_w 6.7/5.7%, $Sr_4Bi_6Se_{13}$ with R_1 8.5%, and $K_2Bi_8S_{13}$ with R/R_w 7.3/8.2%. A number of crystals from many experimental batches were mounted on the diffractometer for data collection. The different data sets of the same compound yielded similar crystallographic results. The ones with the best results are presented in this paper. Data collection parameters and details of structure solution and refinement for all compounds are listed in Table 1. Atomic coordinates and average temperature factors *U*(eq) are listed in Tables 2−4. STRUCTURE TIDY[13] was run to standardize the crystal structure data. Selected bond distances are tabulated in Table 5.

Structure Solutions of $Ba_3Bi_{6.67}Se_{13}$. After data integration, the R_{int} was 0.1966. After applying SADABS[10] to conduct an empirical absorption correction, the R_{int} dropped to 0.0573. The space groups consistent with the observed systematic extinctions are $P2_1/m$ and $P2_1$. The structure was solved by direct methods using SHELX-93.[8] The initial stoichiometry was set to be $Ba_3Bi_7Se_{13}$. After anisotropic refinement in $P2_1/m$, the R_1 and wR_2 values were 0.0644 and 0.1851. The residual electron density was Max = 4.41 e Å^{-3} and Min = −7.62 e Å^{-3}. Because Bi7 had unusually large atomic displacement parameters *U*, its occupancy was refined. The resulting occupancy dropped to 68%. When Ba and Bi were placed at this site and their occupancies were refined simultaneously, the Ba fraction dropped to zero while the Bi fraction stayed

(7) Jones, C. D. W.; Regan, K. A.; DiSalvo, F. J. *Phys. Rev.* **1998**, *B58*, 16057.

(8) (a) Sheldrick, G. M. *SHELXL-93, SHELXL-97*; Institut für Anorganische Chemie der Universität Göttingen: Göttingen, 1993−7. (b) Sheldrick, G. M. *Crystal Structure Refinement-MS DOS 32-Bit Version*, 1993.

(9) Spek, A. L. *Acta Crystallogr.* **1990**, *A46* (Suppl.), C34.

(10) Sheldrick, G. M. *SADABS*; Institut für Anorganische Chemie der Universität Göttingen: Göttingen; the computer program is used by Siemens CCD diffractometers.

(11) (a) Kanatzidis, M. G.; McCarthy, T. J.; Tanzer, T. A.; Chen, L.-H.; Iordanidis, L.; Hogan, T.; Kannewurf, C. R.; Uher, C.; Chen, B.; *Chem. Mater.* **1996**, *8*, 1465−1474. (b) McCarthy, T. J.; Ngeyi, S.; Liao, J.-H.; DeGroot, D. C.; Hogan, T.; Kannewurf, C. R.; Kanatzidis, M. G.; *Chem. Mater.* **1993**, *5*, 331. (c) MaCathy, T. J.; Tanzer, T. A.; Kanatzidis, M. G.; *J. Am. Chem. Soc.* **1995**, *117*, 1294. (d) Chung, D.-Y.; Iordanidis, L.; Rangan, K. K.; Brazis, P. W.; Kannewurf, C. R.; Kanatzidis, M. G. *Chem. Mater.* **1999**, *11*, 1352.

(12) Cordier, G.; Schäfer, H.; Schwidetzky, C. *Rev. Chim. Miner.* **1985**, *22*, 631.

(13) Parthé, E. *STRUCTURE TIDY* program; PC version; University of Geneva: Geneva, 1992.

Table 1. Crystal Data and Structure Refinement of $Ba_3Bi_{6.67}Se_{13}$, $Ba_3Bi_6PbSe_{13}$, and $Ba_3Bi_6SnSe_{13}$

empirical formula	$Ba_3Bi_{6.67}Se_{13}$	$Ba_3Bi_6PbSe_{13}$	$Ba_3Bi_6SnSe_{13}$
formula weight	2831.70	2899.57	2811.07
temperature	293(2) K	168(2) K	158(2) K
wavelength	0.71073 Å	0.71073 Å	0.71073 Å
crystal system	monoclinic	monoclinic	monoclinic
space group	$P2_1/m$ (no. 11)	$P2_1/m$ (no. 11)	$P2_1/m$ (no. 11)
unit cell dimensions	$a = 17.2228(6)$ Å	$a = 17.2427(4)$ Å	$a = 17.2498(5)$ Å
	$b = 4.2729(1)$ Å	$b = 4.2736(1)$ Å	$b = 4.2912(1)$ Å
	$c = 18.4659(6)$ Å	$c = 18.4560(4)$ Å	$c = 18.4590(5)$ Å
	$\alpha = 90°$	$\alpha = 90°$	$\alpha = 90°$
	$\beta = 90.720(0)°$	$\beta = 90.861(1)°$	$\beta = 90.679(1)°$
	$\gamma = 90°$	$\gamma = 90°$	$\gamma = 90°$
volume, Z	1358.8(1) Å^3, 2	1359.84(5) Å^3, 2	1366.28(6) Å^3, 2
density (calculated)	6.921 Mg/m^3	7.081 Mg/m^3	6.833 Mg/m^3
absorption coefficient	64.671 mm^{-1}	66.490 mm^{-1}	60.938 mm^{-1}
$F(000)$	2327	2380	2316
crystal color	black	black	black
crystal size	0.2 × 0.04 × 0.08 mm	0.11 × 0.03 × 0.04 mm	0.15 × 0.02 × 0.03 mm
θ range for data collection	1.10−26.37°	1.10−26.47°	1.10−28.08°
limiting indices	$-21 \le h \le 16$	$-21 \le h \le 21$	$-22 \le h \le 21$
	$-5 \le k \le 5$	$-5 \le k \le 5$	$-5 \le k \le 5$
	$-18 \le l \le 22$	$-23 \le l \le 21$	$-23 \le l \le 20$
reflection collected	7074	9586	11280
independent reflections	2918 ($R_{int} = 0.0573$)	3168 ($R_{int} = 0.1208$)	3428 ($R_{int} = 0.0996$)
absorption Correction	SADABS empirical	SADABS empirical	SADABS empirical
refinement method	full-matrix least-squares on F^2	full-matrix least-squares on F^2	full-matrix least-squares on F^2
data/restraints/parameters	2918/0/140	3166/0/140	3128/6/148
goodness-of-fit on F^2	1.121	1.074	1.188
final R_1/wR_2 [$I > 2\sigma(I)$]	0.0566/0.1393	0.0730/0.1261	0.0634/0.1425
R_1/wR_2 (all data)	0.0765/0.1516	0.1136/0.1527	0.0892/0.1723
extinction coefficient	0.00066(8)	0.00054(6)	0.00065(9)
largest diff. peak and hole	4.487 and −4.083 eÅ^{-3}	3.254 and −5.632 eÅ^{-3}	6.631 and −4.188 eÅ^{-3}
weighting scheme	w^{-1}=[$\sigma^2(F_o^2)$ + (0.0763P)^2 + 0.000P] where P = [max(F_o^2,0) + 2F_c^2]/3	w^{-1} = [$\sigma^2(F_o^2)$ + (0.0333P)^2 + 0.000P] where P = [max(F_o^2,0) + 2F_c^2]/3	w^{-1} = [$\sigma^2(F_o^2)$ + (0.0697P)^2 + 0.000P] where P = [max(F_o^2,0) + 2F_c^2]/3

Table 2. Atomic Coordinates and Equivalent Isotropic Displacement Parameters (Å^2 × 10^3) for $Ba_3Bi_{6.67}Se_{13}$

	x	y	z	U(eq)[a]
Bi(1)	0.8284(1)	1/4	0.3803(1)	17(1)
Bi(2)	0.0811(1)	1/4	0.4226(1)	21(1)
Bi(3)	0.3268(1)	1/4	0.4738(1)	15(1)
Bi(4)	0.1019(1)	1/4	0.0285(1)	23(1)
Bi(5)	0.5092(1)	1/4	0.1190(1)	17(1)
Bi(6)	0.6894(1)	1/4	0.9581(1)	18(1)
Bi(7)	0.0117(1)	1/4	0.7483(1)	16(1)
Ba(8)	0.2637(1)	1/4	0.8246(1)	19(1)
Ba(9)	0.7500(1)	1/4	0.7342(1)	24(1)
Ba(10)	0.4811(1)	1/4	0.6549(1)	16(1)
Se(11)	0.8047(2)	1/4	0.5568(2)	16(1)
Se(12)	0.5779(2)	1/4	0.8232(2)	14(1)
Se(13)	0.0408(2)	1/4	0.5907(2)	14(1)
Se(14)	0.9835(2)	1/4	0.9034(2)	19(1)
Se(15)	0.2759(2)	1/4	0.6425(2)	15(1)
Se(16)	0.3935(2)	1/4	0.9640(2)	16(1)
Se(17)	0.1022(2)	1/4	0.2755(2)	18(1)
Se(18)	0.8127(2)	1/4	0.0560(2)	16(1)
Se(19)	0.3744(2)	1/4	0.3342(2)	14(1)
Se(20)	0.2334(2)	1/4	0.1254(2)	17(1)
Se(21)	0.8695(2)	1/4	0.2379(2)	15(1)
Se(22)	0.6075(2)	1/4	0.2336(2)	15(1)
Se(23)	0.5739(2)	1/4	0.4870(2)	15(1)

[a] U(eq) is defined as one-third of the trace of the orthogonalized U_{ij} tensor.

Table 3. Atomic Coordinates and Equivalent Isotropic Displacement Parameters (Å^2 × 10^3) for $Ba_3Bi_6PbSe_{13}$

	x	y	z	U(eq)[a]
Bi(1)	0.8270(1)	1/4	0.3820(1)	20(1)
Bi(2)	0.0819(1)	1/4	0.4236(1)	20(1)
Bi(3)	0.3271(1)	1/4	0.4744(1)	18(1)
Bi(4)	0.1036(1)	1/4	0.0262(1)	23(1)
Bi(5)	0.5087(1)	1/4	0.1196(1)	20(1)
Bi(6)	0.6883(1)	1/4	0.9590(1)	20(1)
Pb(7)	0.0131(1)	1/4	0.7497(1)	22(1)
Ba(8)	0.2672(1)	1/4	0.8243(1)	19(1)
Ba(9)	0.7478(1)	1/4	0.7343(1)	19(1)
Ba(10)	0.4811(1)	1/4	0.6549(1)	17(1)
Se(11)	0.8026(2)	1/4	0.5571(2)	21(1)
Se(12)	0.5777(2)	1/4	0.8228(2)	20(1)
Se(13)	0.0404(2)	1/4	0.5903(2)	20(1)
Se(14)	0.9814(2)	1/4	0.9074(2)	24(1)
Se(15)	0.2767(2)	1/4	0.6405(2)	17(1)
Se(16)	0.3952(2)	1/4	0.9637(2)	19(1)
Se(17)	0.1062(2)	1/4	0.2763(2)	19(1)
Se(18)	0.8103(2)	1/4	0.0576(2)	19(1)
Se(19)	0.3743(2)	1/4	0.3346(2)	16(1)
Se(20)	0.2354(2)	1/4	0.1246(2)	22(1)
Se(21)	0.8646(2)	1/4	0.2391(2)	21(1)
Se(22)	0.6061(2)	1/4	0.2342(2)	17(1)
Se(23)	0.5731(2)	1/4	0.4872(2)	18(1)

[a] U(eq) is defined as one-third of the trace of the orthogonalized U_{ij} tensor.

around 67%. When both the Bi7 occupancy and its U_{aniso} values were refined at the same time, the Bi7 occupancy went to about 74%, not severely deviating from 67%. Assuming the canonical oxidation states Ba^{2+}, Bi^{3+}, and Se^{2-}, the charge balance condition would require the stoichiometry to be $Ba_3Bi_{6.67}Se_{13}$. Therefore, the Bi7 occupancy was fixed at 0.6667. The R_1 and wR_2 dropped to 0.0566 and 0.1393, respectively. The U values of Bi7 became similar to those of other Bi atoms. The residual peaks were diffusive and within 1 Å of either Ba or Bi. Attempts to solve and refine the structure in $P2_1$ resulted in unacceptable atomic displacement parameters (ADP) and higher R_1/wR_2 values.

Structure Solution of $Ba_3Bi_6PbSe_{13}$. The initial motivation to synthesize $Ba_3Bi_6PbSe_{13}$ was to remove the partial occupancy on the Bi7 site in $Ba_3Bi_{6.67}Se_{13}$ by replacing the trivalent Bi with the divalent Pb. Because the powder X-ray diffraction pattern of $Ba_3Bi_6PbSe_{13}$ is similar to that of Ba_3-

(14) Palmer, D. C. *CrystalDiffract 2.0.0*, 1995.

Table 4. Atomic Coordinates and Equivalent Isotropic Displacement Parameters ($Å^2 \times 10^3$) for $Ba_3Bi_6SnSe_{13}$

	x	*y*	*z*	U(eq)[a]
M(1)[b]	0.8285(1)	1/4	0.3815(1)	13(1)
M(2)[b]	0.0821(1)	1/4	0.4240(1)	10(1)
Bi(3)	0.3259(1)	1/4	0.4759(1)	15(1)
Bi(4)	0.1032(1)	1/4	0.0278(1)	18(1)
M(5)[b]	0.5086(1)	1/4	0.1183(1)	14(1)
Bi(6)	0.6892(1)	1/4	0.9585(1)	15(1)
M(7)[b]	0.0123(1)	1/4	0.7483(1)	16(1)
Ba(8)	0.2658(1)	1/4	0.8248(1)	22(1)
Ba(9)	0.7476(1)	1/4	0.7342(1)	22(1)
Ba(10)	0.4805(1)	1/4	0.6543(1)	14(1)
Se(11)	0.8031(2)	1/4	0.5579(2)	15(1)
Se(12)	0.5773(2)	1/4	0.8221(2)	14(1)
Se(13)	0.0405(2)	1/4	0.5912(2)	14(1)
Se(14)	0.9831(2)	1/4	0.9048(2)	17(1)
Se(15)	0.2760(2)	1/4	0.6425(2)	14(1)
Se(16)	0.3943(2)	1/4	0.9634(2)	16(1)
Se(17)	0.1040(2)	1/4	0.2760(2)	15(1)
Se(18)	0.8123(2)	1/4	0.0562(2)	14(1)
Se(19)	0.3741(2)	1/4	0.3351(2)	14(1)
Se(20)	0.2346(2)	1/4	0.1252(2)	15(1)
Se(21)	0.8685(2)	1/4	0.2379(2)	15(1)
Se(22)	0.6074(2)	1/4	0.2338(2)	14(1)
Se(23)	0.5739(2)	1/4	0.4865(2)	14(1)

[a] *U*(eq) is defined as one-third of the trace of the orthogonalized U_{ij} tensor. [b] M(1): 87(1)% Bi and 13(1)% Sn; M2: 61(1)% Bi and 39(1)% Sn; M(5): 96(1)% Bi and 4(1)% Sn; M(7): 55(1)% Bi and 45(1)% Sn.

$Bi_{6.67}Se_{13}$ and the simulated diffraction pattern (CrystalDiffract 2.0.0)[14] of $Ba_3Bi_6PbSe_{13}$ which has Pb fully occupying the Bi7 site of $Ba_3Bi_{6.67}Se_{13}$, the structure of $Ba_3Bi_6PbSe_{13}$ was refined in $P2_1/m$ starting with the model of $Ba_3Bi_{6.67}Se_{13}$ and Pb placed at the Bi7 site with full occupancy. After anisotropic refinement, no Bi or Pb sites show unusually large *U* values of atomic displacement parameters (ADP). When the occupancies of Bi or Pb sites were refined, the deviation from 1 is less than 1%. It is noteworthy that all cation sites in $Ba_3Bi_6PbSe_{13}$ are fully occupied. Attempts to solve and refine the structure in $P2_1$ or $P2/m$ did not yield an acceptable solution.

In $Ba_3Bi_6PbSe_{13}$, there are seven distinct sites occupied by Bi and Pb, named as *Site n* ($n = 1-7$) hereafter. Because X-ray diffraction cannot distinguish between Pb and Bi, the different ways of distributing Bi and Pb at the seven relevant sites do not result in observable differences in X-ray diffraction patterns and does not cause significant observable changes in atomic parameters or R_1/wR_2. Whether Pb and Bi are randomly distributed or ordered at the seven Bi/Pb sites of *Site n* cannot be unambiguously determined from either our single-crystal or powder X-ray diffraction. However, the plausibility of placing Pb at the Bi7 site is supported by a valence bond calculation (vide infra).

Structure Solution of $Ba_3Bi_6SnSe_{13}$. The crystal structure was initially refined in the model of $Ba_3Bi_6PbSe_{13}$ with Sn replacing for Pb, but the *U* value of Sn at *Site 7* went negative. If full occupancy of Bi at *Site 7* was assumed, the *U* value was unusually large compared with others. Valence calculations suggested that *Site 7* is not purely occupied by a trivalent or a divalent cation (vide infra). As the microprobe analysis suggested a quaternary phase in good agreement with the targeting stoichiometry (Bi/Sn = 5.9 ± 0.6), a hypothetical model with one Sn and six Bi atoms randomly distributed over the seven sites (*Site n*) was tested while maintaining charge balance. The refinement indicated that *Site 7* is occupied by ~55% Bi and 45% Sn. Sn appears on *Site 1*, *2*, and *5* at significant levels, whereas the concentration of Sn on *Site 3*, *4*, and *6* is less than 1%. The final refinement was carried out by restricting *Site 3*, *4*, and *6* fully occupied by Bi but the other four sites occupied by both Sn and Bi. It is worth mentioning that site occupancy is highly correlated with ADP which is in turn influenced by the absorption correction. An empirical absorption correction by using SADABS[10] and an analytical absorption correction by using XPREP[8] were applied. For the face-indexing correction, $R_{int} = 0.0758$, $R_1/wR_2 = 0.0607/0.1478$ ($I > 2\sigma(I)$), gof = 1.726, largest difference peak = 8.323 e/Å^3 and hole = −4.079 e/Å^3. For the SADABS correction, $R_{int} = 0.0996$, $R_1/wR_2 = 0.0634/0.1425$ ($I > 2\sigma(I)$), gof = 1.188, largest difference peak = 6.631e/Å^3 and hole = −4.188 e/Å^3. SADABS[10] produced a smoother Fourier difference map than the analytical absorption correction. Because there was a big peak about 0.5 Å from Ba8 and a hole on Ba8, we put Sn on the difference peak position (Sn8) and constrained the total occupancy of Sn8 and Ba8 to be 1. Ba9 was treated the same way. Sn rather than Ba was assigned to these two positions because their distances to the nearest Se atoms were shorter than 2.86 Å. Using the data set from the analytical absorption correction, we refined the disorder model of Sn8/Ba8 and Sn9/Ba9 to reduce the maxima in the Fourier difference map. The refinement resulted in a Fourier difference map with largest difference peak = 3.433 e/Å^3 and hole = −3.304 e/Å^3, $R_1/wR_2 = 0.0570/0.1393$ ($I > 2\sigma(I)$), and gof = 1.640. This improvement of the reliability factors is small. The occupancies of Sn at the two positions are not significant: 10.1(7)% Sn8 and 8.1(7)% Sn9. Although we cannot exclude the possibility of Ba/Sn disorder, we do not have solid evidence to confirm it. Therefore, the final structure is reported assuming no Ba/Sn disorder. The atomic coordinates are the same within 3σ from the two refinements by the empirical (SADABS[10]) and the analytical absorption corrections; furthermore, the empirical correction yields lower residual densities. Thus the refinement results from the empirical absorption correction by using SADABS[10] are reported here.

Table 5. Selected Bond Lengths [Å] for $Ba_3Bi_{6.67}Se_{13}$, $Ba_3Bi_6PbSe_{13}$, and $Ba_3Bi_6SnSe_{13}$[a]

M(1)−Se(21)	2.732(3)	2.725(4)	2.747(4)
M(1)−Se(15) × 2	2.820(2)	2.813(3)	2.833(2)
M(1)−Se(13) × 2	3.147(2)	3.165(3)	3.152(3)
M(1)−Se(11)	3.289(3)	3.266(4)	3.290(4)
M(2)−Se(17)	2.745(3)	2.756(4)	2.762(4)
M(2)−Se(11) × 2	2.925(2)	2.939(3)	2.937(3)
M(2)−Se(13) × 2	3.002(2)	3.010(3)	3.024(3)
M(2)−Se(13)	3.189(3)	3.169(4)	3.178(4)
M(3)−Se(19)	2.714(3)	2.717(4)	2.738(4)
M(3)−Se(23) × 2	2.825(2)	2.827(3)	2.836(2)
M(3)−Se(11) × 2	3.160(2)	3.142(3)	3.148(3)
M(3)−Se(15)	3.246(3)	3.199(4)	3.203(4)
M(4)−Se(14) × 2	2.890(3)	2.876(3)	2.900(3)
M(4)−Se(20)	2.867(3)	2.888(4)	2.878(4)
M(4)−Se(18) × 2	3.037(2)	3.038(3)	3.031(3)
M(4)−Se(14)	3.063(3)	3.017(4)	3.055(4)
M(5)−Se(22)	2.694(3)	2.680(4)	2.714(3)
M(5)−Se(12) × 2	2.828(2)	2.822(3)	2.836(2)
M(5)−Se(16) × 2	3.128(2)	3.123(3)	3.121(3)
M(5)−Se(16)	3.466(3)	3.455(4)	3.453(4)
M(6)−Se(18)	2.771(3)	2.761(4)	2.770(4)
M(6)−Se(16)	2.954(2)	2.955(3)	2.961(3)
M(6)−Se(20) × 2	2.960(2)	2.957(3)	2.967(3)
M(6)−Se(12)	3.126(3)	3.132(4)	3.154(4)
M(7)−Se(14)	2.911(4)	2.969(4)	2.939(4)
M(7)−Se(13)	2.960(4)	2.987(4)	2.945(4)
M(7)−Se(17) × 2	2.930(2)	3.000(3)	2.968(3)
M(7)−Se(21) × 2	2.967(2)	3.008(3)	2.980(3)
Ba(8)−Se(22) × 2	3.271(3)	3.253(3)	3.257(3)
Ba(8)−Se(21) × 2	3.330(3)	3.318(3)	3.354(3)
Ba(8)−Se(18) × 2	3.351(3)	3.346(4)	3.364(3)
Ba(8)−Se(15)	3.372(4)	3.367(4)	3.366(4)
Ba(8)−Se(16)	3.389(3)	3.398(4)	3.371(4)
Ba(9)−Se(19) × 2	3.268(3)	3.245(3)	3.252(3)
Ba(9)−Se(17) × 2	3.330(3)	3.309(3)	3.347(3)
Ba(9)−Se(20) × 2	3.370(3)	3.378(3)	3.379(3)
Ba(9)−Se(12)	3.407(4)	3.379(5)	3.374(4)
Ba(9)−Se(11)	3.421(4)	3.418(4)	3.402(4)
Ba(10)−Se(19) × 2	3.284(3)	3.287(3)	3.305(3)
Ba(10)−Se(22) × 2	3.349(3)	3.333(3)	3.354(3)
Ba(10)−Se(23) × 2	3.502(3)	3.498(3)	3.491(3)
Ba(10)−Se(23)	3.506(4)	3.498(5)	3.501(4)
Ba(10)−Se(12)	3.508(3)	3.497(4)	3.508(4)
Ba(10)−Se(15)	3.537(3)	3.531(4)	3.532(4)

[a] M stands for Bi/Pb/Sn.

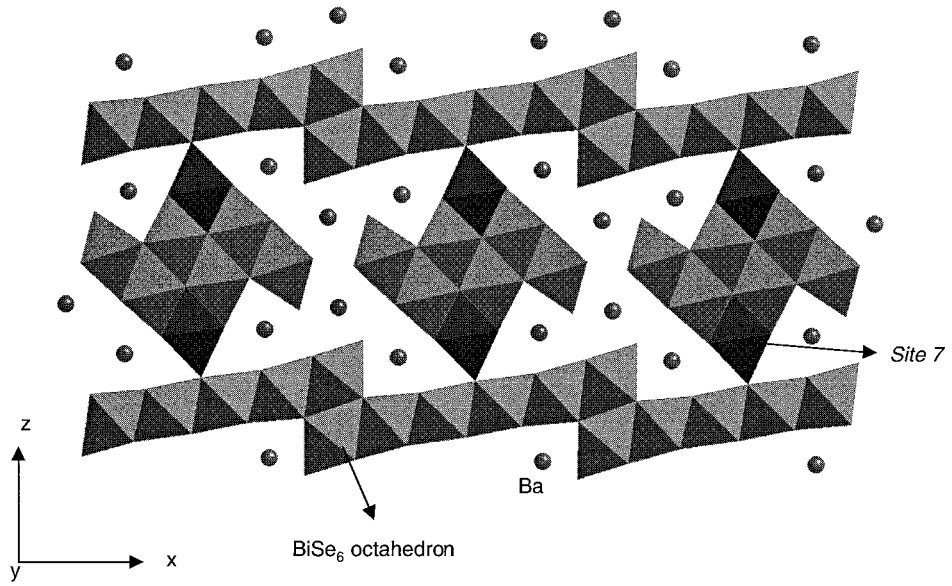

Figure 1. Polyhedral representation of $Ba_3Bi_{6.67}Se_{13}$ viewed along *y* axis showing edge-sharing $BiSe_6$ octahedra. The big gray dots are Ba.

Valence Study. The software package EUTAX (Version 1.2)[15] was run to calculate bond valences and apparent atomic valences. The built-in bond valence parameters were used in the calculation. The maximum distance was set at 4.0 Å.

3. Results and Discussion

Structure Description. Because $Ba_3Bi_{6.67}Se_{13}$, $Ba_3Bi_6PbSe_{13}$ and $Ba_3Bi_6SnSe_{13}$ adopt the same structure type, here the discussion will be focusing on $Ba_3Bi_{6.67}Se_{13}$. The structure type of the three compounds can be viewed as a variant of $Sr_4Bi_6Se_{13}$ with $Bi^{3+}/Pb^{2+}/Sn^{2+}$ at one of the alkaline earth metal sites Sr^{2+}.[12] This structure type is also adopted by $K_2Bi_8S_{13}$[11a] and β-$K_2Bi_8Se_{13}$[4a] which have K^+ and Bi^{3+} occupying the two sites corresponding to Ba8 and Ba9 in $Ba_3Bi_{6.67}Se_{13}$ and $Ba_3Bi_6PbSe_{13}$. The recently reported compound $Ba_{4-x}Bi_{6+2/3x}Se_{13}$ crystallizes in the same structure type.[4d]

Overall, the compound $Ba_3Bi_{6.67}Se_{13}$ can be regarded as a three-dimensional Bi_2Se_3 network disrupted by the insertion of Ba^{2+} with the addition of Se^{2-} to maintain charge balance. The structure of $Ba_3Bi_{6.67}Se_{13}$ has a three-dimensional anionic network $(Bi_{6.67}Se_{13})^{-6}$ with open channels where cations Ba^{2+} fill in as drawn in Figure 1. The anionic network can be described as two interconnecting motifs: infinite slabs parallel to the *xy* plane and interconnecting blocks running along the *y* direction. The two motifs are joined through Bi7. In the space left between the two motifs are the Ba^{2+} ions confined in the tunnels along the *y* direction. All the bismuth atoms are coordinated to six Se atoms to form octahedral $BiSe_6$, which share edges with each other to form the anionic framework (Figure 1). For Bi*n* (n = 1−6), the $BiSe_6$ octahedra are highly distorted; the Bi−Se bond lengths range from 2.694(3) to 3.466(3) Å (Table 5). On the other hand, Bi7 has a less distorted octahedron; the Bi7−Se bond lengths fall between 2.911(4) and 2.967(2) Å. Ba8 and Ba9 are coordinated by eight Se atoms to form bicapped trigonal prisms; Ba10 is coordinated by nine Se atoms to form a tricapped trigonal prism. The structural and bonding characteristics expressed in $Ba_3Bi_{6.67}Se_{13}$ are typical of other Bi/Sb chalcogenides. An extensive discussion of Bi/Sb chalcogenide chemistry can be found in the literature.[11]

In $Ba_3Bi_6PbSe_{13}$, the distribution of Pb and Bi at the seven crystallographically distinct sites is not a simple issue. Single-crystal or powder X-ray diffraction cannot distinguish between Pb and Bi. However, bond-valence analysis may be very effective in distinguishing neighboring atoms in the periodic table. The valence analysis program EUTAX[15,16] assumes the bond valence-bond length equation to be in the "Brown & Altermatt" form: $v(R) = \exp[(R - d)/0.37]$. The built-in single-bond length parameters d were determined as a best fit from the bond lengths of many compounds. In practice, it is common that the calculated apparent valences deviate from true valences, which can be explained by a few factors. For example, bond lengths are influenced not only by valences but also by lone pairs and nonbonding interactions.[16] The apparent valences may appear in a range of values that deviate from the true valences significantly. As a control test, we performed EUTAX calculations on known chalcogenides containing Bi/Pb,[17] for example: PbSe, U_2PbSe_5, $PbPSe_3$, $BaBiSe_3$, and K_3BiSe_3. There is no calculated valence sum exactly equal to integers such as 2 and 3. The Bi sites have valence sums 3.1−3.5 and the Pb sites have valence sums 2.03−2.07. Since bond valence analysis is an empirical method, focusing on the comparison and the overall trends is important in distinguishing neighboring atoms.

Table 6 lists the valence sums at each site of *Site n* (n = 1−7) when they are filled with Pb and when they are filled with Bi. The row of "standard" corresponds to the valence sums when *Site 7* is filled with Pb and the

(15) (a) O'Keeffe, M.; Brese, N. *EUTAX 1.2 program*, 1992. (b) Brese, N. E.; O'Keeffe, M. *Acta Crystallogr.* **1991**, *B47*, 192. (c) O'Keeffe, M.; Brese, N. E. *Acta Crystallogr.* **1992**, *B48*, 152. (c) O'Keeffe, M.; Brese, N. E. *J. Am. Chem. Soc.* **1991** *113*, 3226.

(16) O'Keeffe, M. *Struct. Bond.* **1989**, *71*, 162.

(17) ICSD/RETRIEVE 2.01, Gmelin Institute/Fiz Karlsruhe, Release February 1998.

Table 6. Valence Sums at the Seven Sites in $Ba_3Bi_6PbSe_{13}$ and $Ba_3Bi_6SnSe_{13}$[a]

	Site n						
	1	2	3	4	5	6	7
				$Ba_3Bi_6PbSe_{13}$			
all Bi	3.369	3.227	3.413	3.239	3.427	3.329	2.857
all Pb	2.944	2.819	2.981	2.829	2.994	2.909	2.496
standard	3.369	3.227	3.413	3.239	3.427	3.329	2.496
				$Ba_3Bi_6SnSe_{13}$			
all Bi	3.238	3.177	3.312	3.148	3.291	3.250	3.111
all Sn	2.279	2.236	2.331	2.216	2.316	2.287	2.190

[a] "All Bi", "all Pb", and "all Sn" mean Bi, Pb, and Sn occupying all the seven sites, respectively. "Standard" means the final solution of Pb/Bi distribution adopted in this paper, i.e., Pb on *Site 7* and Bi on the other six sites *Site n* ($n = 1-6$).

other six sites are filled with Bi in $Ba_3Bi_6PbSe_{13}$. Compared with the other six sites, *Site 7* shows the lowest valence sum, and is lower than the other valence sums by almost one unit. From the valence sums in the first two rows, we see that *Site 7* always has a much lower valence sum than the other sites, whether they are occupied by Pb or Bi. From the above observations, it can be inferred that Pb is very likely to occupy only *Site 7*. It is worth mentioning that in $Sr_4Bi_6Se_{13}$, *Site 7* is occupied by Sr^{2+}, a divalent cation.[12]

Assuming that Pb is at *Site 7*, the Pb atom is surrounded by six Se atoms to form an octahedron of $PbSe_6$; its six bond lengths fall between 2.96 and 3.00 Å. The octahedral coordination of $PbSe_6$ is also found in PbSe with a Pb−Se distance at 3.06 Å.[18a] However, in many reported Pb/Se-containing compounds, eight-coordinate Pb is very common with Pb−Se bond distances ranging from 2.95 to 3.50 Å.[18b−e] In $Ba_3Bi_6PbSe_{13}$, the difference of the six bond lengths of Pb−Se is smaller than 0.04 Å, while the difference of bond lengths of Bi−Se around each Bi is bigger than 0.16 Å. The six $BiSe_6$ octahedra are distorted to different extent; and all of them are much more distorted than the $PbSe_6$ octahedron.

Although Pb and Sn belong to the same group, their substitution for Bi and their distribution at the seven sites are different. Not all the Sn goes to *Site 7* in $Ba_3Bi_6SnSe_{13}$. The X-ray refinement shows that *Site 7* is occupied by both Sn (45%) and Bi (55%). Table 6 clearly demonstrates that in $Ba_3Bi_6SnSe_{13}$, the valence sum at *Site 7* is lower than at the other six sites *Site n* ($n = 1-6$), which indicates that *Site 7* may be occupied by Sn. If we compare the valence sums at the seven sites when *Site 7* is occupied by the divalent metal for each compound ($Ba_3Bi_6PbSe_{13}$ and $Ba_3Bi_6SnSe_{13}$), it is interesting to see that the difference of valence sum between *Site 7* and *Site n* ($n = 1-6$) is about 0.03−0.14 in $Ba_3Bi_6SnSe_{13}$, much smaller than the difference 0.73−0.93 in $Ba_3Bi_6PbSe_{13}$. If we compare the valence sums in $Ba_3Bi_6SnSe_{13}$ with those in $Ba_3Bi_6PbSe_{13}$, it is interesting to see that $Ba_3Bi_6SnSe_{13}$ displays lower valence sums at *Site n* ($n = 1-6$) but a higher valence sum at *Site 7* than $Ba_3Bi_6PbSe_{13}$ does. It can be inferred that in $Ba_3Bi_6SnSe_{13}$, Sn may be distributed all over the seven sites but *Site 7* has the highest Sn concentration. It is very likely that *Site 7* is occupied by both Sn and Bi, which is in agreement with the X-ray structural refinement. The empirical absorption correction by using SADABS[10] may lead to errors which keep the *R* values high and make accurate determination of the site occupancies problematic. However, both EUTAX calculations and the structural refinement support mixed occupancy of *Site 7*. Mixed occupancy of other sites *Site n* ($n = 1-6$) must therefore also occur, and the refinement suggests that *Site 1*, *2*, and *5* are most likely candidates.

All the three compounds can be understood in terms of the Zintl−Klemm concept.[19] The assignment of oxidation number is straightforward: Ba^{2+}, Bi^{3+}, Pb^{2+}, Sn^{2+}, and Se^{2-}. The partial occupancy of Bi7 in $Ba_3Bi_{6.67}Se_{13}$ is in agreement with the requirement of charge balance. This prompted us to modify the structure while maintaining charge balance. The synthesis of $Ba_3Bi_6PbSe_{13}$ and $Ba_3Bi_6SnSe_{13}$ was aimed at eliminating the partial occupancy of Bi7. We also attempted to synthesize hypothetical compounds $Ba_2KBi_7Se_{13}$, $BaKCeBi_{6.67}Se_{13}$, and $Ba_2CeBi_5Pb_2Se_{13}$, but the target phases were not obtained. For $Ba_2KBi_7Se_{13}$, $Ba_{3-x}K_xBi_{6.67+x/3}Se_{13}$ ($x = 0.12 \pm 0.04$ by microprobe analysis) was found in the product mixture.

Distortion of Chalcogen Octahedra and Lone Pair $6s^2$. In Bi/Pb chalcogenides, the distortion of the chalcogen octahedra exhibits a wide range. We examined the bond length difference of the longest and the shortest bonds of the six Bi−Q (Q = S, Se) bonds around each Bi/Pb atom in the three isostructural compounds $Ba_3Bi_{6.67}Se_{13}$, $Ba_3Bi_6PbSe_{13}$, and $Ba_3Bi_6SnSe_{13}$. It reveals that among the seven distinct octahedral sites, *Site 5* is the most distorted with 0.74−0.77 Å bond length difference, whereas the octahedron at *Site 7* is almost a regular octahedron with only 0.04−0.05 Å bond length difference. β-$K_2Bi_8Se_{13}$[4a] and $K_2Bi_8S_{13}$[11a] demonstrate the similar pattern.

The above phenomena can be discussed in terms of the stereochemical activity of $6s^2$ lone pair. The lone pairs of electrons $6s^2$ on Pb and Bi may or may not be stereochemically active in compounds, which influences the coordination sphere and brings about interesting structural and electronic properties. Whether the stereochemical activity can be realized structurally depends on the bonding and local environment.[19−22] The expression of stereoactivity of lone pair depends on the mixing of 6s and 6p orbitals and the polarization of the orbitals on Bi or Pb, which is influenced by the local environment. The seven sites of *Site n* in the current structure do not have exactly the same chemical and geometrical environments; therefore at different sites, the stereoactivity of $6s^2$ lone pairs is structurally realized to different degrees.

(18) (a) Noda, Y.; Ohba, S.; Sato, S.; Saito, Y. *Acta Crystallogr.* **1983**, *B39*, 312. (b) Iglesias, J. E.; Steinfink, H. *J. Solid State Chem.* **1973**, *6*, 93. (c) Skowron, A.; Brown, I. D. *Acta Crystallogr.* **1990**, *C46*, 2287. (d) Yun, H.; Ibers, J. A. *Acta Crystallogr.* **1987**, *C43*, 2002. (e) Potel, M.; Brochu, R.; Padiou, J. *Mater. Res. Bull.* **1975**, *10*, 205.

(19) (a) Zintl, E.; Dullenkopf, W. *Z. Phys. Chem.* **1932**, *B16*, 183. (b) Zintl, E.; Brauer, G. *Z. Phys. Chem.* **1933**, *B 20*, 245. (c) Zintl, E. *Angew. Chem.* **1939**, *52*, 1. (d) Klemm, W. *Z. Anorg. Allg. Chem.* **1941**, *247*, 1.

(20) Wheeler, R. A.; Kumar, P. N. V. P. *J. Am. Chem. Soc.* **1992**, *114*, 4776.

(21) (a) Trinquier, G.; Hoffmann, R. *J. Phys. Chem.* **1984**, *88*, 6696. (b) Wang, S.; Mitzi, D.; Landrum, G.; Genin, H.; Hoffmann, R. *J. Am. Chem. Soc.* **1997**, *119*, 724. (c) Rytz, R.; Hoffmann, R. *J. Inorg. Chem.* **1999**, *38*, 1609.

(22) (a) Landrum, G. A.; Hoffmann, R. *Angew. Chem., Int. Ed.* **1998**, *37*, 1887. (b) Landrum, G. A.; Goldberg, N.; Hoffmann, R. *J. Chem. Soc., Dalton Trans.* **1997**, 3605.

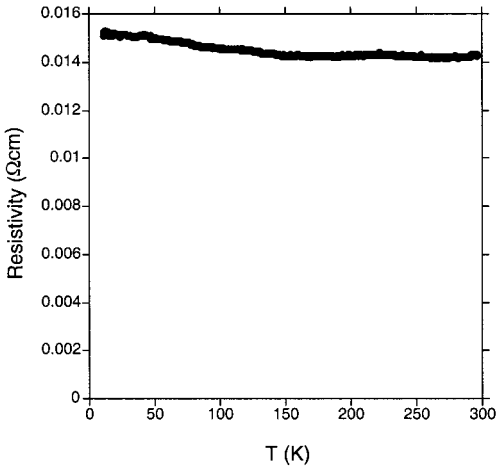

Figure 2. Electrical resistivity ρ versus temperature T measured on the sintered pellet of $Ba_3Bi_{6.67}Se_{13}$.

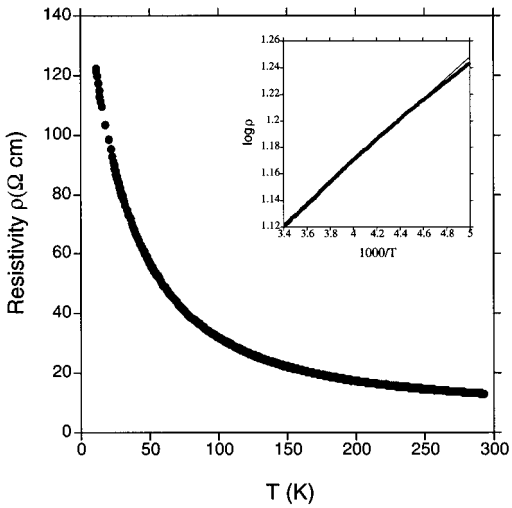

Figure 3. Electrical resistivity ρ versus temperature T measured on the sintered pellet of $Ba_3Bi_6PbSe_{13}$. The inset is a plot of logρ versus $1/T$ for the data above 200 K.

Another way to understand the wide range of distortion is to invoke the language of electron-rich three-center bonds.[22,23] The symmetrical octahedra of [$BiSe_6$] and [$PbSe_6$] can be viewed as classical cases of electron-rich three-center bonding. Similarly, the unsymmetrical ones can be viewed as perturbed three-center systems. The potential energy surfaces for distorting these octahedra are presumably rather flat.[22,23] It allows great flexibility of arranging the local environments (or distorting the octahedral coordination in certain cases) in order to energetically optimize the whole extended structure. This may account the wide spectrum of [BiQ_6] distortion and rich structural chemistry of Bi/Sb chalcogenides.

Transport Properties. In the sample of $Ba_3Bi_{6.67}Se_{13}$, the electrical resistivity ρ (Figure 2) increases only slightly from 0.0143 Ω cm at 296 K to 0.0153 Ω cm at 11 K. The electrical resistivity is higher than that of Bi_2Se_3, $(1.6-2.0) \times 10^{-3}$ Ω cm obtained for single crystals.[24] The high electrical resistivity is characteristic

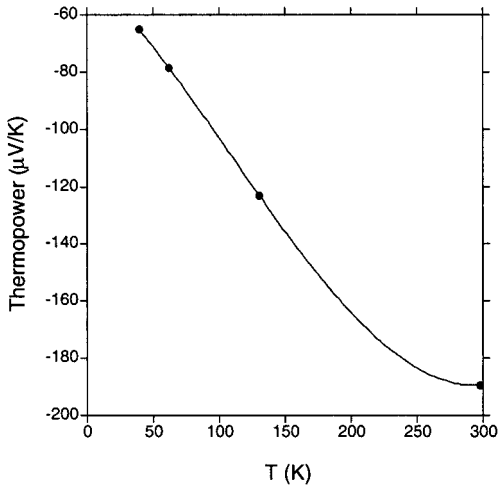

Figure 4. The thermopower versus temperature in $Ba_3Bi_6PbSe_{13}$. For comparison, the thermopower of $Ba_3Bi_{6.67}Se_{13}$ is -70.7 μV/K at 300 K and -35.8 μV/K at 78 K.

of semiconductors. The weak dependence of electrical resistivity on temperature suggests that our $Ba_3Bi_{6.67}Se_{13}$ sample is a degenerate semiconductor. The measured electrical resistivity of $Ba_3Bi_6PbSe_{13}$ (13.25 Ω cm at 292 K) is much higher than that of $Ba_3Bi_{6.67}Se_{13}$. For $Ba_3Bi_6PbSe_{13}$, the plot of ρ versus T (Figure 3) shows behavior typical of a nondegenerate semiconductor; the electrical resistivity increases from about 13 Ω cm at 292 K to 121 Ω cm at 11 K. An activation energy E_a/k_B of 79 K is found by fitting the data above 200 K to $\rho = \rho_0 \exp(-E_a/k_BT)$. The fitting plot of log ρ versus $1/T$ is displayed in the inset of Figure 3.

The thermopower of $Ba_3Bi_{6.67}Se_{13}$ decreases from -70.7 μV/K at 300 K to -35.8 μV/K at 77.8 K. The thermopower of $Ba_3Bi_6PbSe_{13}$ decreases from -189 μV/k at 297 K to -64.8 μV/K at 39 K (Figure 4). The negative sign reveals dominant electron transport in both samples. $Ba_3Bi_6PbSe_{13}$ shows much higher thermopower than $Ba_3Bi_{6.67}Se_{13}$, which is in agreement of the higher resistivity in $Ba_3Bi_6PbSe_{13}$ than in $Ba_3Bi_{6.67}Se_{13}$. The Hall coefficient of $Ba_3Bi_6PbSe_{13}$ was found to be -6.87×10^{-8} (Ω cm)/G, which corresponds to a carrier concentration of $9.0 \times 10^{17} e^-/cm^3$. This may be lower than the optimal doping level for maximum efficiency in a thermoelectric device. Since thermopower S decreases with increasing carrier density and since the thermopower of optimally doped Bi_2Te_3 is above 200 μV/K, this compound does not appear to be competitive with Bi_2Te_3-based thermoelectrics.

Acknowledgment. This work was funded by ONR. We thank Johnson Matthey Electronics for their contribution of elements. We would like to mention the communication and interaction with Professor M. G. Kanatzidis and his group. Y.C.W. thanks Dr. T. P. Braun and Dr. L. Cario for their discussion and suggestion. Y.C.W. appreciates Emil B. Lobkovsky for his help in performing X-ray single crystal diffraction data collection and using relevant software.

Supporting Information Available: Tables of anisotropic thermal parameters of all atoms and bond angles of the three title compounds; listings of observed and calculated structure factor for the three titled compounds. This material is available free of charge via the Internet at http://pubs.acs.org.

CM990571U

(23) Albright, T. A.; Burdett, J. K.; Whangbo, M. H. *Orbital Interaction in Chemistry*; Wiley: New York, 1985; Chapter 14.
(24) Black, J.; Conwell, E. M.; Seigle, L.; Spencer, C. W. *J. Phys. Chem. Solids* **1957**, *2*, 240.